



## Riparian evapotranspiration shapes stream flow dynamics and water budgets in a Mediterranean catchment

**Authors:** Anna Lupon<sup>1</sup>, José L. J. Ledesma<sup>2</sup>, Susana Bernal<sup>3,4</sup>

### **Affiliations:**

5 <sup>1</sup> Department of Forest Ecology and Management, Swedish University of Agricultural Sciences (SLU).  
Skogsmarksgränd, 901 83 Umeå, Sweden.

<sup>2</sup> Department of Aquatic Sciences and Assessment, Swedish University of Agricultural Sciences (SLU).  
Lennart Hjelms väg 9, SE, 750 07 Uppsala, Sweden.

10 <sup>3</sup> Departament de Biologia Evolutiva, Ecologia i Ciències Ambientals, Universitat de Barcelona. Av.  
Diagonal 643, 08028 Barcelona, Spain.

<sup>4</sup> Integrative Freshwater Ecology Group, Center for Advanced Studies of Blanes (CEAB-CSIC). Accés a  
la Cala Sant Francesc 14, 17300 Blanes, Spain.

*Correspondence to:* Anna Lupon ([anna.lupon@slu.se](mailto:anna.lupon@slu.se))



## 15 Abstract

Riparian trees can regulate stream flow dynamics and water budgets by taking up large amounts of water from both soil and groundwater compartments. However, their role has not been fully recognized in the hydrologic literature and the catchment modeling community. In this study, we explored the influence of riparian evapotranspiration (ET) on stream flow by simulating daily stream exports from three nested  
20 Mediterranean sub-catchments, both including and excluding the riparian compartment in the structure of the PERSiST rainfall-runoff model. The model goodness of fit significantly improved with the inclusion of the riparian compartment, especially during the vegetative period when, according to our simulations, riparian ET reduced mean daily stream flow by 26%. Moreover, sensitivity analyses suggested that riparian ET was a significant hydrological process contributing to stream flow recession in summer. At  
25 the catchment scale, simulated riparian ET accounted for 7% of annual water depletions, its contribution being especially noticeable during summer (8–19%). Simulations considering future climate change scenarios suggest that longer vegetative periods would result in higher contribution of riparian ET to annual water budgets. Annual increases in riparian ET ranged between 2 and 13% from the most conservative to the most extreme drought scenarios. Overall, our results highlight that a good assessment  
30 of riparian ET is essential for understanding catchment hydrology and stream flow dynamics in Mediterranean regions. Thus, the inclusion of the riparian compartment in hydrological models is strongly recommended in order to establish proper management strategies in water-limited regions.

**Keywords:** PERSiST model, riparian evapotranspiration, water resources, stream flow, Mediterranean regions, climate change, aridity index.



## 35 1 Introduction

Precipitation and upland tree evapotranspiration (ET) are considered the two most important components controlling annual water budgets in catchment hydrology. This conceptualization is supported by the fact that, in most regions, landscape units other than uplands (e.g. riparian zones) occupy a small percentage of the catchment area (< 3%) (Tockner and Stanford, 2002). However, empirical studies have shown that  
40 riparian ET can influence stream flow dynamics by lowering groundwater levels and increasing groundwater residence times (Bernal et al., 2004; Burt et al., 2002). In water limited regions, water demand by riparian trees can influence the exchange of water between terrestrial and fluvial ecosystems by disconnecting saturated soils from streams and promoting the displacement of stream water towards the riparian zone (Butturini et al., 2003; Lupon et al., 2016; Rassam et al., 2006). Altogether, these studies  
45 suggest that hydrological processes occurring in the riparian zone, specifically those induced by riparian ET, can be critical to understand stream flow dynamics in regions potentially suffering from water scarcity. Yet, most of these studies have been conducted at plot or reach scales and there are still few exercises assessing the influence of riparian ET on stream flow and water exports at the catchment scale.

Riparian trees can play an important role in catchment water budgets because their water requirements  
50 are generally high compared to upland tree species (Baldocchi and Ryu, 2011; Doody and Benyon, 2011). Yet, the contribution of riparian ET to catchment annual water budgets varies widely among biomes (from 0% to > 30%) depending on the amount of water available for vegetation (Dahm et al., 2002; Cadol et al., 2012; Contreras et al., 2011). In tropical systems, for instance, soil water content is usually high in both upland and riparian zones, and hence, these two compartments show similar ET rates (2–5 mm d<sup>-1</sup>; Cadol  
55 et al., 2012; da Rocha et al., 2004). Conversely, in arid systems, riparian zones stay relatively wet compared to upland areas and can support ET rates between 1 and 7 mm d<sup>-1</sup>, as much as one order of magnitude higher than those in the surrounding upland (0.1–0.4 mm d<sup>-1</sup>; Dahm et al., 2002; Kurc and Small, 2004). These differences among biomes suggest that the potential of riparian forests to shape stream flow dynamics and water budgets likely increases with increasing water scarcity.

60 Mediterranean catchments are unique natural laboratories for evaluating the influence of riparian ET on stream and catchment hydrology as well as to test the response of riparian ET to changes in climatic



drivers, namely temperature and precipitation. Mediterranean regions exhibit marked seasonal patterns in both hydrology and vegetative activity, and they hold an intermediate position in the climatic gradient, which makes them especially vulnerable to future changes in climate (IPCC, 2013). Previous studies have shown that capturing abrupt changes in groundwater tables associated with summer riparian ET are essential to predict daily and seasonal shifts in stream flow in Mediterranean areas (Lupon et al., 2016; Medici et al., 2008). Thus, a better understanding of the implications of these hydrological processes on catchment water budgets and on water availability for both in- and off-stream uses is needed. This information is critical to assess the hydrological management of Mediterranean forested catchments as well as to achieve feasible predictions of hydrological and ecological responses to future climate.

The aim of this study was to explore the role of riparian ET on regulating present and future stream flow dynamics and catchment water exports in a Mediterranean forested headwater catchment on a seasonal and annual basis. To do so, we used the rainfall-runoff model PERSiST (Precipitation, Evapotranspiration and Runoff Simulator for Solute Transport; Futter et al., 2014) to reproduce the observed stream hydrographs at three nested sub-catchments along which the area covered by riparian forests varied from 0 to 10%. We expected that the influence of riparian ET on stream flow dynamics and catchment water exports will be magnified during late spring and summer, when hydrological connectivity between uplands and the stream network is low. Moreover, we simulated different climate scenarios for the region in order to explore changes in the relative contribution of riparian ET to total catchment water budgets with increasing drying.

## 2 Study site

The Font del Regàs catchment is located in the Montseny Natural Park, NE Spain (41°50'N, 2°30'E). The climate is subhumid Mediterranean, with mild winters, wet springs, and dry summers. Annual precipitation is  $925 \pm 151$  mm (mean  $\pm$  SD), less than 1% falling as snow. Mean annual temperature averages  $12.1 \pm 2.5$  °C (period 1940–2000, Catalan Metereologic Service).

Total catchment area is 14.2 km<sup>2</sup> and its altitude ranges from 500 to 1500 m above the sea level (a.s.l.) (Figure 1). The geology is dominated by biotitic granite and the topography includes steep slopes (28%)



(Institut Cartografic de Catalunya, 2010). Evergreen oak forests (*Quercus ilex*) cover the lower part of the catchment (54% of the catchment area), whereas the upper part is covered mainly by deciduous European beech (*Fagus sylvatica*) forests and heathlands (38 and 2% of the catchment area, respectively) (Figure 1). Upland soils (pH ~ 6) are sandy, with a 3 cm deep O horizon followed by a 5 to 15 cm deep A horizon. The riparian forest covers 6% of the total catchment area and it is relatively flat (slope < 10%). Riparian width increases from 6 to 28 m along the catchment and the total basal area of riparian trees increases by 12-fold. Black alder (*Alnus glutinosa*), European ash (*Fraxinus excelsior*), black locust (*Robinia pseudoacacia*), and black poplar (*Populus nigra*) are the most abundant tree species in the riparian forest, with a basal area of 14, 4, 3 and 2 m<sup>2</sup> ha<sup>-1</sup>, respectively. Riparian soils (pH ~ 7) are sandy-loam, with a 5 cm deep organic layer followed by a 30 cm deep A horizon.

For this study, we selected three nested sub-catchments along a 5.6 km stretch of the Font del Regàs stream (Figure 1, Table 1). The upstream sub-catchment (800–1500 m a.s.l, local drainage area 1.8 km<sup>2</sup>) was mostly composed by beech forest (93%) and had no riparian forest. Vegetation in the midstream sub-catchment (650–800 m a.s.l, local drainage area 6.74 km<sup>2</sup>) included both oak (52.5%) and beech (42.5%) forests. The stream at the midstream sub-catchment had a wetted width of 2–3 m and was flanked by a mixed forest (5%, 5–15 m wide) of *Alnus glutinosa* and *Fraxinus excelsior*. The downstream sub-catchment (500–650 m a.s.l, local drainage area 4.42 km<sup>2</sup>) was mainly covered by oak forest (58%) and, to a lesser extent, by beech forest (32%). The stream at the downstream sub-catchment had a wetted width of 3–3.5 m and was flanked by a well-developed riparian forest (10%, 15–30 m wide) consisting mainly of *Robinia pseudoacacia*, *Populus nigra*, and *Alnus glutinosa*.

### 3 Materials and methods

#### 3.1 The PERSiST model

PERSiST is a conceptual, semi-distributed, bucket-type model that simulates daily catchment water fluxes (Futter et al., 2014). The flexible model framework allows representing the runoff generation process as a specified number of vertically and horizontally interconnected buckets (representing soil layers) within a mosaic of landscape units. In this way, PERSiST allows differentiating the riparian compartment from



115 other catchment water pools (see below). The riparian water fluxes represented in the model are  
subsurface flow and evapotranspiration (Futter et al., 2014).

In the model, rainfall is directed to the stream as overland flow or infiltrated to the upper soil layer. Vertically, water can move to lower soil layers via infiltration or return to the atmosphere via ET. Horizontally, soil water moves downhill to other catchment compartments or, alternatively, to the stream. Water movement is controlled by field capacities, hydrological connectivity, and infiltration-related parameters. Water lost via ET is landscape unit-specific and is controlled by degree day rates and threshold temperature parameters. During dry conditions, (i) an ET adjustment parameter can be used at the soil layer level to limit ET and (ii) a specified fraction of the incoming rainfall can be directly transported to stream runoff. Rainfall can also be intercepted by the canopy. The magnitude and flashiness of the simulated flow is also dependent on the catchment area and water velocity-related parameters. Catchment and landscape unit-specific rain multipliers correct for potential rainfall measurement biases. Finally, landscape unit-specific parameter values are used to specify the fraction of water moving between contiguous soil layers and with the stream at every time step.

### 3.2 Model input data and configuration

We used PERSiST to explore the influence of riparian ET on the seasonal variation of stream flow at Font del Regàs. We calibrated PERSiST for two complete hydrological years (Sep 2010–Aug 2012) at the outlet of the up-, mid-, and downstream sub-catchments using as input data time series of daily precipitation (in mm) and mean daily air temperature (in °C). Both precipitation and temperature were recorded at 15-min intervals at a meteorological station located at the valley bottom of the catchment (Figure 1) and converted to daily values for model simulation. At each sub-catchment outlet, stream water level was monitored at 15-min intervals using a water pressure sensor connected to an automatic sample (Model 1612, Teledyne Isco) (Figure 1). An empirical relationship between stream flow (in  $L s^{-1}$ ) and stream water level was obtained using the slug chloride addition method in the field ( $n = 57, 60,$  and  $61$  for up-, mid-, and downstream sub-catchments, respectively; in all cases:  $R^2 > 0.97$ ; Lupon et al., 2016). Daily accumulated flows considering the total upstream drainage area at the three locations were used for model calibration. Model simulation was started in January 2010 to have an 8-month warm-up period.



To investigate the importance of riparian ET to the temporal pattern of stream flow at Font del Regàs, we calibrated the model for the three sub-catchment outlets (referred as to “stream sites” hereafter) both including and excluding the riparian compartment in the model structure. The aim was to determine whether riparian ET improved the goodness of fit between observed and simulated stream flow. In the first model configuration (not including a riparian compartment), we used a simple one-compartment approach to represent the catchment area in all three sub-catchments (i.e., a single upland representation). For each sub-catchment, the upland compartment was divided into two landscape units representing evergreen and deciduous forests in appropriate proportions (Table 1), and the soil was divided into three layers representing overland (quick), upper (soil), and lower (groundwater) strata.

The second model configuration consisted on both an upland and a riparian compartment, which was added for the mid- and downstream sub-catchments (5 and 10% area covered by riparian forest, respectively) (Table 1). In this configuration, the upper upland layer communicated downhill with the riparian layer and vertically with the groundwater. The riparian layer also received water inputs from groundwater, which was shared for both upland and riparian compartments. The stream received water inputs from both the riparian compartment and the groundwater. Following knowledge of the area, overland flow was not used in either model configuration or all water entering the overland (quick) bucket percolated to the upper soil layer either in the upland or riparian compartments. ET was simulated from uplands and riparian layers separately. The importance of riparian ET on simulating stream water flow and catchment water budgets was determined by comparing specific statistical metrics of goodness of fit (see below) from the two model configurations (including and excluding the riparian compartment).

### 3.3 Calibration procedure

Model calibration was done manually for all six model instances (3 sub-catchments x 2 model configurations) in order to (i) match ET values reported for the different forest types (“soft calibration”) and (ii) optimize a combination of statistical metrics (i.e. model efficiency) that compare simulated and observed flows (“hard calibration”). Note that the instances from the upstream site were equivalent in the two configurations because this sub-catchment had no riparian forest. Manual calibration has been proved as a robust method for obtaining acceptable simulations within the Integrated Catchment (INCA) family



of models, of which PERSiST is the common hydrological model (Cremona et al., 2017; Futter et al., 2014; Ledesma et al., 2012).

170 For the soft calibration, the parameterization of both upland and riparian ET was adjusted to obtain values  
of water demand within the ranges reported for evergreen forest (i.e. evergreen oak; 550–650 mm yr<sup>-1</sup>),  
deciduous forest (i.e. beech; 600–750 mm yr<sup>-1</sup>), and riparian forests (i.e. poplar, alder and ash; 750–1000  
mm yr<sup>-1</sup>) at Montseny or nearby (< 50 km) mountains (Àvila et al., 1996; Folch and Ferrer, 2015; Llorens  
and Domingo, 2007; Sabater and Bernal, 2011). We calibrated the model assuming (i) a higher ET from  
175 evergreen forest than from deciduous and riparian forests during the dormant period and (ii) a higher  
riparian ET than evergreen and deciduous ET during the vegetative period. The first assumption was  
based on the premise that deciduous trees cannot transpire during the dormant period, while the second  
assumption was based on the idea that riparian trees are closer to water sources, and thus, they are not as  
water limited as upland trees (both evergreen oak and beech) in summer. Other parameterization  
180 requirements during soft calibration included matching reported annual canopy rainfall interception  
values for similar forest types (Àvila et al., 1996; Terradas, 1984; Terradas and Savé, 1992) and a rainfall  
correction for south- and north-facing slopes which roughly corresponded to evergreen and deciduous  
forests, respectively (Piñol et al., 1992).

For the hard calibration, model parameters related to water fluxes, including the fraction of water  
185 communicating soil layers and time constants (a proxy for hydrological connectivity), were adjusted to  
optimize the Nash and Sutcliffe (NS) efficiency index (important to fit high flows), the log NS (important  
to fit low flows), the relative volume differences of observed versus simulated stream flow (RVD)  
(important to maintain the water balance), and the overall graphical fit between observed and simulated  
hydrographs. For both NS and log(NS), higher values indicate a better goodness of fit. For RVD, positive  
190 and negative values indicate that the model under- and overestimated the stream flow, respectively. The  
three indexes (NS, log(NS), and RVD) were estimated for the six model instances for the whole data set  
as well as for the riparian vegetative (April–October) and dormant (November–March) periods separately.





### 3.4 Model validation and sensitivity analysis

195 To validate the model, we compared monthly mean values of riparian ET simulated with PERSiST with those obtained empirically from daily stream flow variations. Daily variations of stream flow can be used as a proxy for ET from near-stream zones (Cadol et al., 2012; Gribovszki et al., 2010) and they correlate well with direct sap flow measurements at the study site (Lupon et al., 2016). Daily stream flow variations measured at one particular point integrates riparian ET upstream from that point. Thus, we assumed that differences in specific daily stream flow variations between the up- and midstream sites, and the mid- and downstream sites were comparable to the specific riparian ET simulated with PERSiST for the midstream and downstream sub-catchments, respectively.

205 Once the best parameter set was obtained for the model configuration that included the riparian compartment, we further investigated the importance of riparian ET on regulating stream flow at Font del Regàs by using a Monte Carlo (MC) sensitivity analysis approach. This approach consisted in comparing sets of model efficiencies obtained from two MC analyses. In the first one, all model parameters potentially influencing stream flow were allowed to vary  $\pm 25\%$  with respect to the best performing parameter set from manual calibration (non-fixed ET analysis, Table S1). In the second one, landscape specific ET-related parameters (i.e. degree day rates, threshold temperatures, and ET adjustments) were kept constant, while the other parameters were again allowed to vary  $\pm 25\%$  (fixed ET analysis, Table S1). Fixed ET-related parameters were set to the mean optimal values obtained for each landscape unit after the manual calibration. The MC analyses consisted of 100 iterations of 1000 runs each. We used Tukey's Honestly Significant Difference tests (Tukey HSD) to compare  $\log(NS)$  obtained from the 100 best runs (each from each of the iterations) between the fixed and non-fixed ET analyses. A decrease in the goodness of fit (i.e. lower values of  $\log(NS)$ ) for the fixed ET analysis was interpreted as an indication that the outputs of the model were sensitive to riparian ET, and thus, that the riparian component was important for simulating stream flow dynamics. The comparison between fixed and non-fixed ET analyses was made for the downstream site only, first for the overall calibration period, and then for the vegetative and dormant periods separately.



### 3.5 Modelling future projections of water budgets

220 The best manual parameterization of the model configuration including the riparian compartment was  
used to simulate future changes in catchment water budgets and to explore the contribution of riparian ET  
to these changes. We calculated future water balances considering predicted changes in climate for 2081–  
2100. Daily meteorological data for the period 1933–2000 was available from Turó de l'Home  
meteorological station, located < 10 km from Font del Regàs meteorological station (Meteocat,  
225 [www.meteocat.cat](http://www.meteocat.cat)). Although Turó de l'Home is usually colder and wetter than Font del Regàs, monthly  
precipitation and temperature showed a strong correlation between the two stations for the period 2010–  
2014 (in the two cases:  $R^2 > 0.90$ ,  $p < 0.001$ ,  $n > 53$ , Figure S1). The linear regression models for these  
two sites were used to construct daily time series of temperature and precipitation at Font del Regàs for  
both the reference period (1981–2000) and the future period (2081–2100) based on Representative  
230 Concentration Pathway (RCP) projections.

RCP projections provided by IPCC (2013) are based on the reference period 1986–2005. We assumed  
similar projections values for our reference period (1981–2000), which was the one for which data at Turó  
de l'Home was available. We applied the 2.5, 4.5, 6.0, and 8.5 RCP scenarios for Mediterranean zones  
including percentiles 0.25, 0.50, and 0.75 (IPCC, 2013). In general, RCP scenarios forecast an increase  
235 in temperature all year round, but more pronounced in summer than in winter. Precipitation is predicted  
to decrease in April–September, while small changes are expected in October–March (Table 2).

For each year and RCP scenario, we calculated (i) the Aridity Index (AI) as a proxy of water availability  
(UNEP, 1992), and (ii) the relative contribution of simulated riparian ET to annual water catchment  
depletions at the whole catchment scale (i.e. the sum of simulated upland ET, riparian ET, and stream  
240 flow at the downstream site). The AI is the relationship between annual precipitation and potential ET  
(PET), which was estimated using the Penman-Monteith equation on daily time steps (Allen et al., 1998).  
We assumed constant wind velocity ( $1 \text{ m s}^{-1}$ ) and relative humidity (75%) in the equation because these  
data were not recorded at the Turó de l'Home meteorological station. These assumptions were based on  
a 5-year time series of meteorological data at the Font del Regàs catchment (period 2010–2014; wind  
245 velocity =  $1.0 \pm 0.4 \text{ m s}^{-1}$ ; relative humidity =  $75 \pm 9\%$ ). We examined the relationship between the



relative contribution of riparian ET to annual water catchment depletions and AI by fitting a two segment piecewise linear regression model. All the statistical analyses were carried out with the R 3.3.0 statistical software (R Core Team, 2012).

## 4 Results

### 250 4.1 Data–model fusion

For the calibration period (2010–2012), mean annual flow was  $23 \pm 17$ ,  $82 \pm 66$ , and  $105 \pm 113$  L s<sup>-1</sup> at the up-, mid-, and downstream sites, respectively. The three sites showed the same seasonal pattern, characterized by a strong decline in stream flow during the vegetative period (Figure 2). The model configuration excluding the riparian compartment successfully reproduced the magnitude and seasonal pattern of stream flow at the three sampling sites (Table 3 and Figure 2). However, there were mismatches between simulated and observed values, especially during the vegetative period, when stream flows were overestimated at the three sampling sites (RVD < 0, Table 3). The mismatches were especially noticeable in the downstream site, where simulated values were, on average, 53% higher than observed ones (Table 3).

260 The efficiency indexes indicated that the inclusion of the riparian compartment was essential to improve the agreement between simulated and observed flows at the mid- and downstream sites. The model including the riparian compartment showed higher NS and log(NS) metric values and RDV values closer to 0 (more accurate stream water volumes) than the one without riparian compartment (Table 3). Moreover, the model including the riparian compartment captured both the magnitude and seasonal pattern exhibited by stream flow even during low flow periods (Figure 2). On average, the inclusion of the riparian compartment reduced daily stream flow by 27% during the vegetative period at the downstream site (Table 3).

### 265 4.2 Model validation and sensitivity analysis

There was a good agreement between simulated daily rates of riparian ET and those obtained independently of model outputs for both the mid- and downstream sub-catchments. Simulated rates of

270



riparian ET were lower during the dormant ( $0.89 \pm 0.97 \text{ mm d}^{-1}$ ) than during the vegetative period ( $3.7 \pm 1.3 \text{ mm d}^{-1}$ ). The lowest simulated ET values occurred in January and February ( $0.1\text{--}0.3 \text{ mm d}^{-1}$ ), while June and August showed the highest ones ( $5\text{--}7 \text{ mm d}^{-1}$ ) (Figure S2). The daily variation of stream flow followed a seasonal pattern similar to that exhibited by simulated daily riparian ET. Consequently, there was a strong and positive relationship between monthly mean values of simulated daily riparian ET and measured daily stream flow variations for both the midstream sub-catchment (linear regression [l.r.],  $R^2 = 0.83$ ,  $p < 0.001$ ,  $n = 24$ ) and the downstream sub-catchment (l.r.,  $R^2 = 0.88$ ,  $p < 0.001$ ,  $n = 24$ ) (Figure 3).

The sensitivity analysis showed no differences in log(NS) values between the analysis with fixed and non-fixed ET parameters for the whole calibration period (Figure 4). The same occurred when comparing fixed and non-fixed ET simulations for the dormant period. For the vegetative period, the simulation of stream flow worsen when the ET parameters were fixed as indicated by the decrease in log(NS) efficiencies (Figure 4). Similar results were obtained for the NS metric (not shown).

#### 4.3 Present and future contribution of riparian ET to catchment water budgets

Simulated rates of riparian ET averaged  $931 \text{ mm yr}^{-1}$  for the calibration period (2010–2012) and contributed 5.91% to annual water losses. This contribution falls within the range of simulated values (5.54–8.42%) obtained for the reference period (1981–2000; mean annual riparian ET =  $862 \pm 105 \text{ mm}$ ). During both calibration and reference periods, the contribution of riparian ET to water catchment depletion was maximal from July to September, when it accounted for 8–19% of water catchment losses.

According to our simulations, mean annual riparian ET will increase in the future by 2% (scenario RCP 2.5 percentile 0.25) to 13% (scenario RCP 4.5 percentile 0.75), reaching mean annual rates of riparian ET between 879 and 977  $\text{mm yr}^{-1}$ . This will represent an increase in the contribution of riparian ET to catchment water budgets of 1–2% compared to the reference period (Table 4). Moreover, future increases in warming and drying will smooth the seasonality of riparian ET by lengthening the vegetative period (ET rates  $> 0 \text{ mm d}^{-1}$ ) by 6 to 106 days (depending on the scenario and year) (Figure 5).



In the most moderate scenario (RCP 2.5 percentile 0.5), mean daily riparian ET values increased by  $0.3 \pm 0.1 \text{ mm d}^{-1}$  during the dormant period, which represents an increase of  $19 \pm 7 \%$  compared to the reference period. During the vegetative period, the projected changes in mean daily riparian ET were smaller ( $-0.1 \pm 0.1 \text{ mm d}^{-1}$ ) and represent a small fraction compared to the reference period ( $-2 \pm 4 \%$ ) (Figure 5a and 5b). The most extreme scenario (RCP 8.5, percentile 0.5) simulated high riparian ET rates ( $> 2 \text{ mm d}^{-1}$ ) during most of the year. For this scenario, riparian ET rates increased by  $0.6 \pm 0.1 \text{ mm d}^{-1}$  during the dormant period, which represents an increase of  $46 \pm 16 \%$  compared to the reference period. During the vegetative period, riparian ET rates decreased by  $-0.4 \pm 0.6 \text{ mm d}^{-1}$ . This is a decrease of  $11 \pm 22 \%$  compared to the reference period (Figure 5g and 5h).

The AI decreased from  $0.65 \pm 0.18$  to  $0.45 \pm 0.15$  between the reference and the most extreme climate scenario (RCP 8.5, percentile 0.75). The contribution of riparian ET to catchment water budgets was low ( $6.40 \pm 0.35 \%$ ) and unrelated to AI for  $\text{AI} > 0.83$ . Below this threshold, the contribution of riparian ET to catchment water budgets increased linearly up to 9.78% with decreasing AI. This dual behavior was well captured by a two segment linear regression relating AI and riparian ET contribution to catchment water depletion with a break point at  $\text{AI} = 0.83$  ( $R^2 = 0.77$ ,  $p < 0.001$ ,  $n = 260$ ) (Figure 6).

## 5 Discussion

### 5.1 Influence of riparian ET on stream flow and catchment water budgets

This study shows that the riparian zone contributed to regulate water exports and budgets at the Font del Regàs catchment. The inclusion of the riparian compartment in the PERSiST model structure improved the simulations, especially at the downstream site, where the riparian zone occupies 10% of the catchment area. These results support the idea that riparian zones are especially important on shaping stream flow dynamics at the valley bottom of mountainous catchments, likely due to the combination of a lower catchment connectivity (i.e. lower water inputs from uplands) (Bernal et al., 2012; Covino and McGlynn, 2007) and a greater water demand by riparian trees (Lupon et al., 2016).

In agreement with our expectations, the influence of the riparian zone on stream flow dynamics varied between seasons. During the dormant period, the model efficiencies barely improved when the riparian



compartment was included in PERSiST (< 5%), suggesting a minimal effect of the riparian zone on stream flow dynamics (Table 3). Conversely, the riparian zone played a key role during the vegetative period because it contributed to drying up the stream as shown by the notable improvement in the log(NS) index, which is a proxy of the goodness of fit during low flow conditions. Moreover, mismatches between simulated and observed water volumes decreased substantially (by 26%) if riparian ET was included, suggesting that the riparian zone can be important to regulate low flows in this catchment (Table 3). Although the inclusion of the riparian compartment contributed to significantly improve the goodness of fit, the model was not able to capture the lowest flows at the end of the vegetative period. Hydrological processes not included so far in the PERSiST structure, such as the uptake of water by trees directly from the stream (Gribovszki et al., 2010; Tabacchi et al., 2000) or the reverse flux of water from the stream towards the riparian zone (Butturini et al., 2003; Rassam et al., 2006), could contribute to drop down stream flow at Font del Regàs, and therefore to the mismatches between observed and simulated flows. These hydrological processes have been shown to be relevant for reproducing stream flow dynamics in Mediterranean and semiarid areas (e.g. Medici et al. 2008), and thus PERSiST could improve its ability to simulate stream flows in water limited catchments if these processes would be implemented in the model structure.

The sensitivity analysis indicated that riparian ET was an important hydrological process driving stream flow during the vegetative period because the model efficiency (log(NS) index) was significantly higher when riparian ET parameters were allowed to vary. Moreover, our results suggest that the hydrological processes occurring in the riparian compartment could reduce daily stream flow by 48% during the vegetative period. This value is consistent with previous studies showing that riparian ET can reduce the amount of water entering to streams by 30–100% (Dahm et al., 2002; Folch and Ferrer, 2015; Kellogg et al., 2008; Lupon et al., 2016). Previous models have suggested that the transpiration process from saturated riparian zones is essential to successfully represent the annual water balance of water-limited catchments (Medici et al., 2008; Tsang et al., 2014). On an annual basis, our simulations indicate that riparian ET can account for ~ 7% of annual catchment depletions at Font del Regàs (Table 4). The contribution of riparian ET to water budgets was especially noticeable during the dry period of the year, when it contributed as much as 19% to daily catchment depletions. These values are similar to those



350 estimated for other catchments with  $AI = 0.6\text{--}0.8$  (Folch and Ferrer, 2015; Tsang et al., 2014; Wine and Zou, 2012; Yeh and Famiglietti, 2008) and suggest that computations of catchment water budgets neglecting riparian ET will overestimate catchment water resources.

Overall, PERSiST was able to successfully simulate stream flow dynamics in the studied Mediterranean catchment, regardless of whether the model structure included or not the riparian compartment ( $\log(NS) > 0.81$ ,  $RDV < 0.11$ ). Moreover, the validation analysis supported the simulation results because the model was able to successfully capture both the magnitude and the temporal patterns of riparian water demand estimated with an independent empirical approach (Figure 3). The successful simulations obtained for Font del Regàs provide evidence that PERSiST can be an appropriate tool for understanding catchment hydrology as well as for exploring how specific hydrological processes, such as riparian ET, can influence stream hydrology under different climatic conditions and future scenarios.

## 360 **5.2 Future changes in riparian ET**

Our simulations suggest that changes in climate projected for later in this century will influence both the magnitude and temporal pattern of riparian ET rates in Font del Regàs. Riparian ET rates will decrease in June–September and increase in November–May. Simulated decreases in riparian ET during the vegetative period were related to lower soil water availability as a consequence of lower precipitation in summer. In concordance, other studies in water-limited regions have shown that low ET rates in summer could result from the disconnection between the water table and the active root zone depth (Baird and Maddock, 2005; Serrat-Capdevila et al., 2007), which can accelerate leaf litter fall (Rood et al., 2008; Sabater and Bernal, 2011) and promote stream desiccation (Medici et al., 2008; Serrat-Capdevila et al., 2007).

On the other hand, the overall warmer temperatures predicted for winter months explain the projected increase of riparian ET during this period. According to our simulations, the length of the vegetative period could increase by 6 to 106 days depending on the applied scenario, mostly as a consequence of an earlier onset of the leaf out period. The enlargement simulated by PERSiST is consistent with observations of spring advancement reported in forests worldwide (e.g. Peñuelas and Boada, 2003;



Richardson et al., 2006) and strongly supports the idea that climate change has a marked effect on tree phenology. Our results also suggest that the effect of lengthening of the vegetative period will overwhelm the reduction of ET rates during summer, and that this change in seasonality will increase annual riparian water use by 2–13%. This warming-induced pattern is concordant with that reported for water-limited riparian forests in southern USA (Bunk, 2012; Serrat-Capdevila et al., 2011).

Finally, we found that increases in annual riparian ET under a warmer climate may have a small effect (1–2%) on the relative contribution of riparian ET to annual catchment water budgets. The small effect predicted by the model was likely because warming also induced higher ET from upland forests ( $4 \pm 11\%$ ). However, our hydrological model does not account for changes in vegetation community induced by warming, a phenomenon that is expected to occur in areas experiencing increases in water stress (Benito-Garzón et al., 2008; García-Arias et al., 2014; Peñuelas and Boada, 2003, Walther et al., 2002). If water becomes limiting, especially in the upland environments, species capable to better adjust their evapotranspirative demand may be favored and become dominant (Engelbrecht et al., 2007), which would lead to decreases in ET from uplands compared to riparian zones. In fact, previous studies suggest that the contribution of riparian ET to catchment water depletion can increase disproportionately with water limitation, and that a threshold exists at intermediate arid positions (i.e. AI = 0.8) (Lupon et al., 2016). Below this threshold, the contribution of riparian ET to water budgets can markedly increase up to 40%, though riparian zones usually occupy less than 10% of the total catchment area (Tockner and Stanford, 2002). Our simulations are in line with this idea and further suggest that riparian forests could switch from energy-limited to water-limited systems as warming and drying increases in the future (Budyko, 1974; Creed et al., 2014).

## 6 Conclusions and Implications

This study highlights that riparian ET can influence stream flow dynamics and water budgets in Mediterranean catchments. We showed that including the riparian zone within the PERSiST model configuration led to improved model efficiencies and more accurate simulation of stream flow dynamics, especially during summer. On an annual basis, riparian ET contributed by 7% to water catchment depletions, its contribution being especially noticeable (8–19%) during dry summer months. Our results





add to the growing body of knowledge showing that riparian hydrology is essential for understanding and predicting stream flow dynamics in catchments experiencing some degree of water limitation. Moreover, our climate simulations indicated that riparian ET could play a major role on catchment water budgets as water scarcity increases in the future. At Font del Regàs, for instance, projected decreases of annual stream flow by the end of this century (3–13%) could be accompanied by increases in riparian ET of the same order (2–13%). Similar predictions have been made for other water-limited catchments of America and Europe (Christensen et al., 2004; Rood et al., 2008; Serrat-Capdevila et al., 2007), forewarning the potential increase of ecological issues related to water scarcity in regions that are already water limited. Overall, this study highlights that the ecohydrology of riparian zones needs to be considered for a responsible management and conservation of water resources in Mediterranean catchments.

## Acknowledgments

We are thankful to Sílvia Poblador, Andrew Wade, and Martin Erlandsson for their invaluable field and modelling assistance. Special thanks are extended to Martyn Futter for his inspirational contributions. Financial support was provided by the Spanish Government through the projects MONTES-Consolider (CSD2008-00040-MONTES), MEDFORESTREAM (CGL2011-30590), and MEDSOUL (CGL2014-59977-C3-2). AL was supported by a Kempe Foundation stipend (Sweden). JLJL was funded by the Swedish Research Council (Svenska Forskningsrådet Formas, Grant/Award Number: 2015-1518). SB work was funded by the Spanish Research Council (JAE-DOC027), the Spanish CICT (Juan de la Cierva contract JCI-2008-177), European Social Funds (FSE), and the NICUS (CGL-2014-55234-JIN) project.

## References

- Allen, R. G., Pereira, L. S., Raes, D., and Smith, M.: Crop evapotranspiration - Guidelines for computing crop water requirements, *FAO Irrig. Drain. Pap.*, 56, 1–15, 1998.
- Àvila, A., Neal, C. and Terradas, J.: Climate change implications for streamflow and streamwater, *J. Hydrol.*, 177, 99–116, doi:10.1016/0022-1694(95)02789-0, 1996.



- Baird, K. J. and Maddock, T.: Simulating riparian evapotranspiration: a new methodology and application for groundwater models, *J. Hydrol.*, 312, 176–190, doi:10.1016/j.jhydrol.2005.02.014, 2005.
- 430 Baldocchi, D. D. and Ryu, Y.: A synthesis of forest evaporation fluxes -from days to years- as measured with Eddy covariance, in *Forest Hydrology and Biogeochemistry*, edited by D. F. Levia, D. Carlyle-Moses, and T. Tanaka, pp. 101–116, Springer Netherlands, Dordrecht., 2011.
- Benito-Garzón, M., Sánchez de Dios, R. and Sainz-Ollero, H.: Effects of climate change on the distribution of Iberian tree species, *Appl. Soil Ecol.*, 11, 169–178, doi:10.3170/2008-7-18348, 2008.
- 435 Bernal, S., Butturini, A., Riera, J. L., Vázquez, E. and Sabater, F.: Calibration of the INCA model in a Mediterranean forested catchment: the effect of hydrological inter-annual variability in an intermittent stream, *Hydrol. Earth Syst. Sci.*, 8, 729–741, 2004.
- Bernal, S., von Schiller, D., Martí, E. and Sabater, F.: In-stream net uptake regulates inorganic nitrogen export from catchments under base flow conditions, *J. Geophys. Res. Biogeosciences*, 117, 1–10, doi:10.1029/2012JG001985, 2012.
- 440 Budyko, M. I.: *Climate and Life*, Volume 18, edited by Budyko, Academic Press, New York., 1974.
- Bunk, D.: Changing demands from riparian evapotranspiration and free-water evaporation in the lower Colorado River basin under different climate scenarios, *Doctoral Thesis*, 2012.
- 445 Burt, T. P., Pinay, G., Matheson, F. E., Haycock, N. E., Butturini, A., Clément, J.-C., Danielescu, S., Dowrick, D. J., Hefting, M. M., Hillbricht-Ilkowska, A. and Maître, V.: Water table fluctuations in the riparian zone: Comparative results from a pan-European experiment, *J. Hydrol.*, 265, 129–148, doi:10.1016/S0022-1694(02)00102-6, 2002.
- Butturini, A., Bernal, S., Nin, E., Hellin, C., Rivero, L., Sabater, S. and Sabater, F.: Influences of the stream groundwater hydrology on nitrate concentration in unsaturated riparian area bounded by an intermittent Mediterranean stream, *Water Resour. Res.*, 39, 1–13, doi:10.1029/2001WR001260, 2003.



- 450 Cadol, D., Kampf, S. and Wohl, E.: Effects of evapotranspiration on baseflow in a tropical headwater catchment, *J. Hydrol.*, 462–463, 4–14, doi:10.1016/j.jhydrol.2012.04.060, 2012.
- Christensen, N. S., Wood, A. W., Voisin, N., Lettenmaier, D. P. and Palmer, R. N.: The effects of climate change on the hydrology and water resources of the Colorado River Basin, *Climatic Chang.*, 62, 337–363, 2004.
- 455 Contreras, S., Jobbágy, E. G., Villagra, P. E., Noretto, M. D. and Puigdefábregas, J.: Remote sensing estimates of supplementary water consumption by arid ecosystems of central Argentina, *J. Hydrol.*, 397, 10–22, doi:10.1016/j.jhydrol.2010.11.014, 2011.
- Covino, T. P. and McGlynn, B. L.: Stream gains and losses across a mountain-to-valley transition: Impacts on watershed hydrology and stream water chemistry, *Water Resour. Res.*, 43, W10431, 460 doi:10.1029/2006WR005544, 2007.
- Creed, I. F., Spargo, A. T., Jones, J. A., Buttle, J. I. M. M., Mary, B., Beall, F. D., Booth, E. G., Campbell, J. L., Clow, D., Elder, K., Green, M. B., Grimm, N. B. and Miniati, C.: Changing forest water yields in response to climate warming: results from long-term experimental watershed sites across North America, *Glob. Chang. Biol.*, 20, 3191–3208, doi:10.1111/gcb.12615, 2014.
- 465 Cremona, F., Vilbaste, S., Couture, R.-M., Nõges, P. and Nõges, T.: Is the future of large shallow lakes blue-green? Comparing the response of a catchment-lake model chain to climate predictions, *Clim. Change*, 141, 347–361, doi:10.1007/s10584-016-1894-8, 2017.
- Dahm, C. N., Cleverly, J. R., Coonrod E. Allred, J., Thibault, J. R., McDonnell, D. E. and Gilroy, D. J.: Evapotranspiration at the land/ water interface in a semi-arid drainage basin, *Freshw. Biol.*, 47, 831–844, 470 2002.
- Doody, T. and Benyon, R.: Quantifying water savings from willow removal in Australian streams, *J. Environ. Manage.*, 92, 926–935, doi:10.1016/j.jenvman.2010.10.061, 2011.



- 475 Engelbrecht, B. M. J., Comita, L. S., Condit, R., Kursar, T. A., Tyree, M. T., Turner, B. L. and Hubbell, S. P.: Drought sensitivity shapes species distribution patterns in tropical forests, *Nature Letters*, 447, 80–83, doi:10.1038/nature05747, 2007.
- Folch, A. and Ferrer, N.: The impact of poplar tree plantations for biomass production on the aquifer water budget and base flow in a Mediterranean basin., *Sci. Total Environ.*, 524–525, 213–24, doi:10.1016/j.scitotenv.2015.03.123, 2015.
- 480 Futter, M. N., Erlandsson, M. A., Butterfield, D., Whitehead, P. G., Oni, S. K. and Wade, A. J.: PERSiST: a flexible rainfall-runoff modelling toolkit for use with the INCA family of models, *Hydrol. Earth Syst. Sci.*, 18, 855–873, doi:10.5194/hess-18-855-2014, 2014.
- García-Arias, A., Francés, F., Moreales-de la Cruz, M., Real, J., Vallés-Morán, F., Garófano-Gómez, G. and Martínez-Capel, F.: Riparian evapotranspiration modelling: Model description and implementation for predictiong vegetation spatial distribution in semi-arid environments, *Ecohydrology*, 7, 659–677, 485 doi:10.1002/eco.1387, 2014.
- Gribovszki, Z., Szilágyi, J. and Kalicz, P.: Diurnal fluctuations in shallow groundwater levels and streamflow rates and their interpretation – A review, *J. Hydrol.*, 385, 371–383, doi:10.1016/j.jhydrol.2010.02.001, 2010.
- Institut Cartografic de Catalunya: Orthophotomap of Catalunya 1:25 000. Generalitat de Catalunya. 490 Departament de Política Territorial i Obres, 2010.
- IPCC: Summary for Policymakers, in *Climate Change 2013: The Physical Science Basis.*, edited by Stocker and V. B. and P. M. M. T.F., D. Qin, G.-K. Plattner, M. Tignor, S.K. Allen, J. Boschung, A. Nauels, Y. Xia, Cambridge University Press, Cambridge, United Kingdom., 2013.
- 495 Kellogg, D. Q., Gold, A. J., Groffman, P. M., Stolt, M. H. and Addy, K.: Riparian groundwater flow patterns using flownet analysis: evapotranspiration-induced upwelling and implications for N removal, *J. Am. Water Resour. Assoc.*, 44, 1024–1034, doi:10.1111/j.1752-1688.2008.00218, 2008.



- Kurc, S. A. and Small, E. E.: Dynamics of evapotranspiration in semiarid grassland and shrubland ecosystems during the summer monsoon season, central New Mexico, *Water Resour. Res.*, 40, W09305, doi:10.1029/2004WR003068, 2004.
- 500 Ledesma, J. L. J., Köhler, S. J. and Futter, M. N.: Long-term dynamics of dissolved organic carbon: Implications for drinking water supply, *Sci. Total Environ.*, 432, 1–11, doi:10.1016/j.scitotenv.2012.05.071, 2012.
- Llorens, P. and Domingo, F.: Rainfall partitioning by vegetation under Mediterranean conditions. A review of studies in Europe, *J. Hydrol.*, 335, 37–54, doi:10.1016/j.jhydrol.2006.10.032, 2007.
- 505 Lupon, A., Bernal, S., Poblador, S., Martí, E. and Sabater, F.: The influence of riparian evapotranspiration on stream hydrology and nitrogen retention in a subhumid Mediterranean catchment, *Hydrol. Earth Syst. Sci.*, 20, 3831–3842, doi:10.5194/hess-20-3831-2016, 2016.
- Medici, C., Butturini, A., Bernal, S., Vázquez, E., Sabater, F. Vélex, J. I. and Francés, F.: Modelling the non-linear hydrological behaviour of a small Mediterranean forested catchment, *Hydrol. Process.*, 3828, 510 3814–3828, doi:10.1002/hyp, 2008.
- Peñuelas, J. and Boada, M.: A global change-induced biome shift in the Montseny mountains (NE Spain), *Glob. Chang. Biol.*, 9, 131–140, 2003.
- Piñol, J., Àvila, A., Escarré, A., Lledó, M. J. and Rodà, F.: Comparison of the hydrological characteristics of three small experimental holm oak forested catchments in NE Spain in relation to larger areas, 515 *Vegetatio*, 99–100, 169–176, 1992.
- R Core Team: R: A language and environment for statistical computing, [online] Available from: <http://www.r-project.org/>, 2012.
- Rassam, D. W., Fellows, C. S., De Hayr, R., Hunter, H. and Bloesch, P.: The hydrology of riparian buffer zones; two case studies in an ephemeral and a perennial stream, *J. Hydrol.*, 325, 308–324, 520 doi:10.1016/j.jhydrol.2005.10.023, 2006.



Richardson, A. D., Schenck Bailey, A., Denny, E. G., Martin, C. W. and O’Keefe, J.: Phenology of a northern hardwood forest canopy, *Glob. Chang. Biol.*, 12, 1174–1188, doi:10.1111/j.1365-2486.2006.01164.x, 2006.

525 da Rocha, H. R., Goulden, M. L., Miller, S. D., Menton, M. C., Pinto, L. D. V. O., de Freitas, H. C. and Silva Figueira, A. M.: Seasonality of water and heat fluxes over a tropical forest in eastern Amazonia, *Ecol. Appl.*, 14, 22–32, 2004.

Rood, S. B., Pan, J., Gill, K. M., Franks, C. G., Samuelson, G. M. and Shepherd, A.: Declining summer flows of Rocky Mountain rivers: Changing seasonal hydrology and probable impacts on floodplain forests, *J. Hydrol.*, 349, 397–410, doi:10.1016/j.jhydrol.2007.11.012, 2008.

530 Sabater, F. and Bernal, S.: Keeping healthy riparian and aquatic ecosystems in the Mediterranean: challenges and solutions through riparian forest management, in *Water for forests and people in the Mediterranean*, edited by Y. Boirot, C. Gracia, and M. Palahí, pp. 151–155., 2011.

535 Serrat-Capdevila, A., Valdés, J. B., González-Pérez, J., Baird, K., Mata, L. J. and Maddock, T.: Modeling climate change impacts – and uncertainty – on the hydrology of a riparian system: The San Pedro Basin (Arizona/Sonora), *J. Hydrol.*, 347, 48–66, doi:10.1016/j.jhydrol.2007.08.028, 2007.

Serrat-Capdevila, A., Scott, R. L., Shuttleworth, W. J. and Valdés, J. B.: Estimating evapotranspiration under warmer climates: Insights from a semi-arid riparian system, *J. Hydrol.*, 399, 1–11, doi:10.1016/j.jhydrol.2010.12.021, 2011.

540 Tabacchi, E., Lambs, L., Guillo, H., Planty-Tabacchi, A.-M., Muller, E. and Décamps, H.: Impacts of riparian vegetation on hydrological processes, *Hydrol. Process.*, 14, 2959–2976, 2000.

Terradas, J.: *Introducció a la ecologia del faig en el Montseny*, Diputació., 1984.

Terradas, J. and Savé, R.: The influence of summer and winter stress and water relationship on the distribution of *Quercus ilex* L., *Vegetatio*, 99–100, 137–145, 1992.



- 545 Tockner, K. and Stanford, J. A.: Riverine flood plains: present state and future trends, *Environ. Conserv.*, 29, 308–330, doi:10.1017/S037689290200022X, 2002.
- Tsang, Y., Hornberger, G., Kaplan, L. A., Newbold, J. D. and Aufdenkampe, A. K.: A variable source area for groundwater evapotranspiration : impacts on modeling stream flow, *Hydrol. Process.*, 28, 2439–2450, doi:10.1002/hyp.9811, 2014.
- UNEP: World Atlas of Desertification, *World Atlas Desertif.*, 69, 1992.
- 550 Walther, G., Post, E., Convey, P., Menzel, A., Parmesan, C., Beebee, T. J. C., Fromentin, J., I, O. H. and Bairlein, F.: Ecological responses to recent climate change, *Nature*, 416, 389–395, 2002.
- Wine, M. L. and Zou, C. B.: Long-term streamflow relations with riparian gallery forest expansion into tallgrass prairie in the Southern Great Plains, USA, *For. Ecol. Manage.*, 266, 170–179, doi:10.1016/j.foreco.2011.11.014, 2012.
- 555 Yeh, J.-F. and Famiglietti, J.: Regional groundwater evapotranspiration in Illinois, *J. Hydrometeorol.*, 10, 464–478, doi:10.1175/2008JHM1018.1, 2008.



## Tables and Figures

560

**Table 1** Catchment drainage area, percentage of evergreen oak, deciduous beech and riparian forest area, width of the riparian zone, and total basal area of riparian trees for the three nested sub-catchments considered in this study.

	Sub-catchment characteristics				Riparian zone characteristics	
	Local drainage area (km <sup>2</sup> )	Evergreen (%)	Deciduous (%)	Riparian (%)	Mean Width (m)	Total Basal Area (m <sup>2</sup> BA)
<b>Upstream</b>	1.80	8.2	92.8	0.0	--	--
<b>Midstream</b>	6.74	52.6	42.5	4.9	12	822
<b>Downstream</b>	4.42	57.8	32.3	9.9	19	1354





565 **Table 2** Representative Concentration Pathway (RCP) projections for Mediterranean zones for 2081–  
 2100 as compared with the reference period 1981–2000. RCP values are indicated for each season for  
 temperature and for each semester for precipitation. Values are medians and interquartile ranges [25<sup>th</sup>,  
 75<sup>th</sup> percentiles] (IPCC, 2013).

Projection	Temperature (°C)				Precipitation (%)	
	Dec–Feb	Mar–May	June–Aug	Sep–Nov	Oct–Mar	Apr–Sep
<b>RCP 2.5</b>	+1.25 [+0.75, +1.25]	+0.75 [+0.75, +1.25]	+1.25 [+0.75, +1.75]	+1.25 [+0.75, +1.75]	0 [0, +5]	0 [-5, 0]
<b>RCP 4.5</b>	+1.75 [+1.25, +2.50]	+1.75 [+1.25, +2.50]	+2.50 [+1.75, +3.5]	+2.50 [+1.75, +2.50]	0 [-5, +5]	0 [-15, 0]
<b>RCP 6.0</b>	+1.75 [+1.75, +2.50]	+2.50 [+1.75, +2.50]	+3.50 [+2.50, +4.50]	+2.50 [+2.50, +3.50]	-5 [-15, 0]	-5 [-15, 0]
<b>RCP 8.5</b>	+3.50 [+2.50, +4.50]	+3.50 [+3.50, +4.50]	+6.00 [+4.50, +6.00]	+4.50 [+3.50, +6.00]	-5 [-15, 0]	-25 [-35, -15]

570



575

**Table 3** Comparison between model calibrations including and excluding the riparian compartment. Log transformed Nash-Sutcliffe (NS) model efficiency coefficient and relative volume differences (RDV) of observed versus simulated stream flow (in parenthesis) at the up-, mid-, and downstream sites for vegetative, dormant, and whole calibration periods (September 2010–August 2012). Negative RDV values indicate an overestimation of modelled flow volumes compared to observed flow volumes, while positive RDV values indicate the opposite. The NS model efficiency values are not shown because they were similar to log(NS) values.

	Vegetative		Dormant		All data	
	No Riparian	Riparian	No Riparian	Riparian	No Riparian	Riparian
<b>Upstream</b>	0.56 (-0.19)	0.56 (-0.19)	0.82 (0.16)	0.82 (0.16)	0.82 (0.01)	0.82 (0.01)
<b>Midstream</b>	0.56 (-0.20)	0.70 (-0.07)	0.87 (0.15)	0.89 (0.12)	0.85 (0.09)	0.89 (0.04)
<b>Downstream</b>	0.00 (-0.53)	0.49 (-0.27)	0.90 (0.12)	0.91 (0.07)	0.81(-0.11)	0.88 (-0.05)

580



**Table 4** Aridity index, annual riparian evapotranspiration (ET) rates, and relative contribution of riparian ET to annual catchment water depletions (i.e., upland ET + riparian ET + stream flow) for the reference period (1981–2000) and for each Representative Concentration Pathway (RPC) scenario during the future period (2081–2100). Values are mean  $\pm$  standard deviation.

Scenario	Percentile	Aridity Index	Annual Riparian ET (mm)	Riparian ET Contribution (%)
<b>Reference</b>		0.65 $\pm$ 0.19	862 $\pm$ 105	7.09 $\pm$ 0.89
<b>RCP 2.5</b>	0.25	0.62 $\pm$ 0.20	879 $\pm$ 115	7.36 $\pm$ 0.93
	0.50	0.63 $\pm$ 0.20	910 $\pm$ 116	7.42 $\pm$ 0.94
	0.75	0.64 $\pm$ 0.20	936 $\pm$ 124	7.42 $\pm$ 0.93
<b>RCP 4.5</b>	0.25	0.59 $\pm$ 0.16	848 $\pm$ 120	7.67 $\pm$ 0.98
	0.50	0.60 $\pm$ 0.19	922 $\pm$ 128	7.68 $\pm$ 0.96
	0.75	0.62 $\pm$ 0.20	977 $\pm$ 136	7.68 $\pm$ 0.94
<b>RCP 6.0</b>	0.25	0.52 $\pm$ 0.14	826 $\pm$ 117	7.96 $\pm$ 0.96
	0.50	0.58 $\pm$ 0.16	934 $\pm$ 126	7.78 $\pm$ 0.93
	0.75	0.56 $\pm$ 0.18	969 $\pm$ 135	7.82 $\pm$ 0.93
<b>RCP 8.5</b>	0.25	0.50 $\pm$ 0.17	759 $\pm$ 132	8.25 $\pm$ 0.96
	0.50	0.53 $\pm$ 0.18	862 $\pm$ 145	8.16 $\pm$ 0.95
	0.75	0.45 $\pm$ 0.15	952 $\pm$ 160	8.22 $\pm$ 0.91

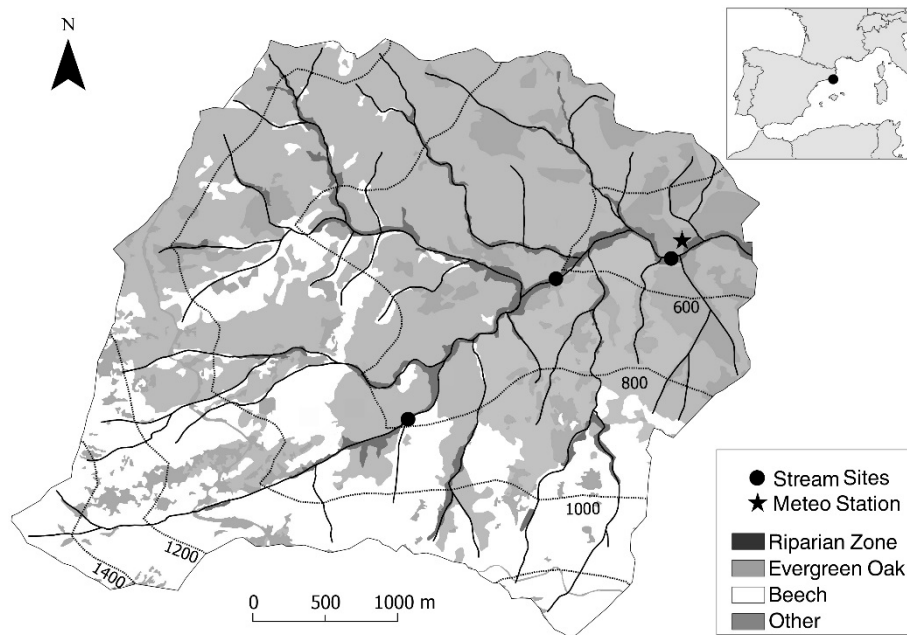


**Figure 1** Map of the Font del Regàs catchment (Montseny Natural Park, NE Spain). The location of the three nested stream sites (black circles) and the meteorological station where precipitation and temperature was measured (star) are shown.

595

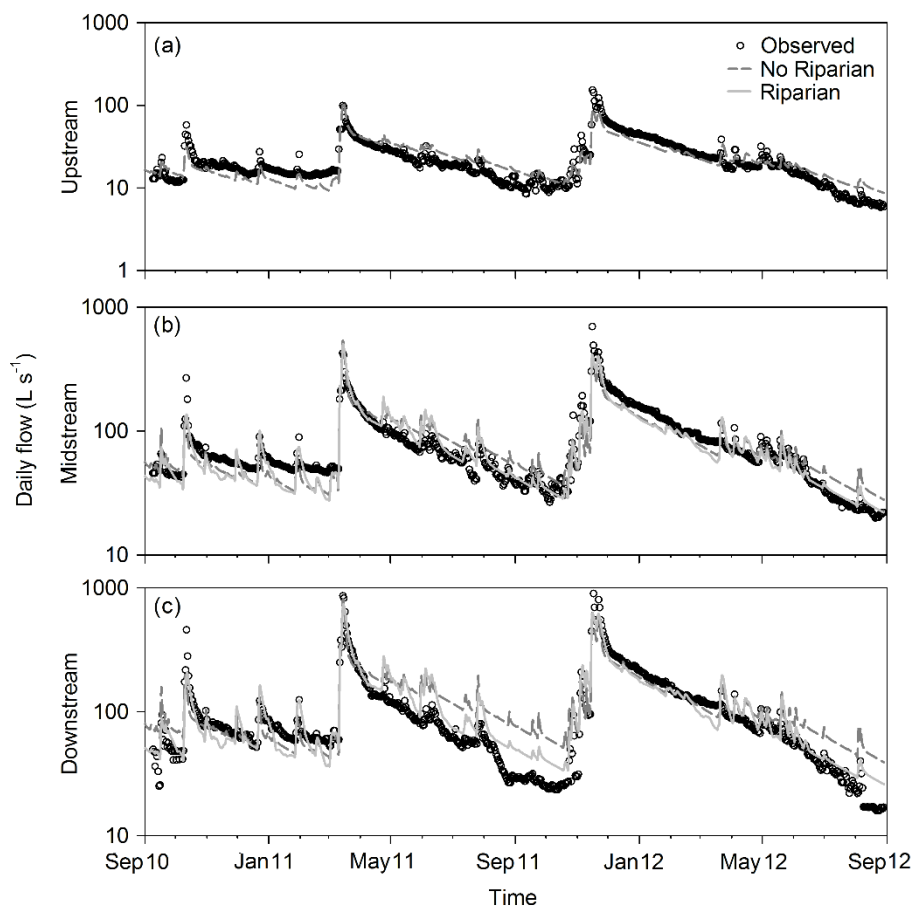
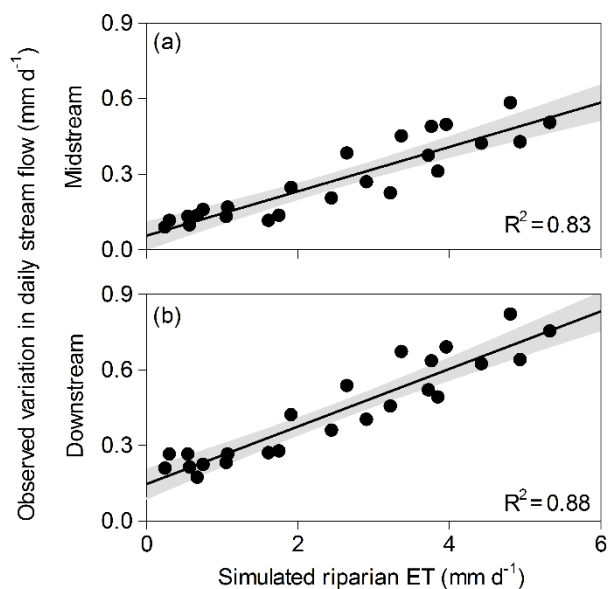


**Figure 2** Temporal pattern of stream flow for the (a) upstream, (b) midstream, and (c) downstream sites during the study period. Open circles represent observed values, while lines are simulated values excluding (dashed) and including (solid) the riparian compartment in the model configuration. Note that the upstream sub-catchment had no riparian forest, and therefore, simulations with and without riparian zone are equal.

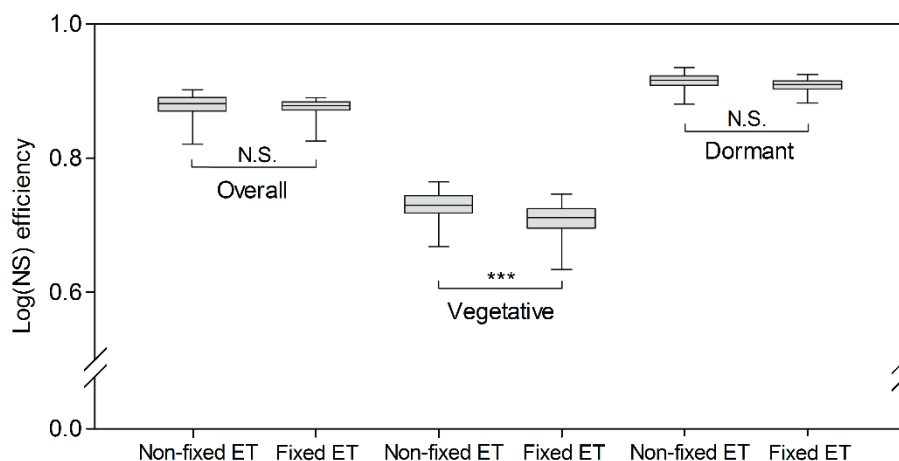
600



605

**Figure 3** Relationship between monthly mean values of simulated daily riparian evapotranspiration (ET) and observed daily stream flow variations (used here as an independent proxy of riparian ET) for (a) the midstream and (b) the downstream sub-catchments for the calibration period (September 2010–August 2012). The linear regression and the 95% confidence interval are also shown. For both mid- and downstream sites: p-value < 0.001, n = 24. The upstream sub-catchment had no riparian forest and it is not shown.

610



615 **Figure 4** Box plot of the 100 best log(NS) efficiencies obtained with the Monte Carlo (MC) simulations  
using the model configuration that included the riparian compartment at the downstream sub-catchment.  
MC analyses were performed using all potentially sensitive parameters first (Non-fixed ET), and fixing  
evapotranspiration-related parameters second (Fixed ET). Means of corresponding distribution pairs were  
compared using Tukey's Honestly Significant Difference tests. N.S. indicate no significant difference and  
620 \*\*\* indicate statistically significant difference ( $p < 0.0001$ ).

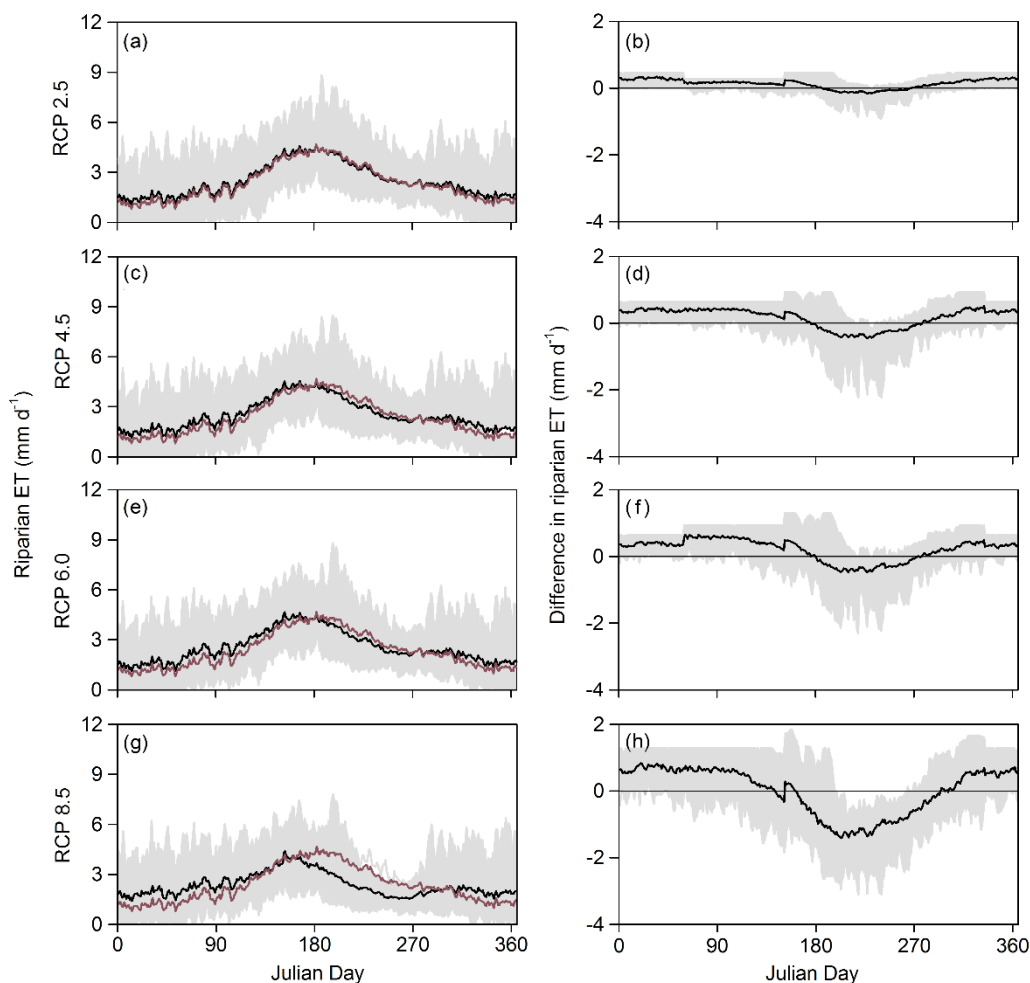


**Figure 5** Seasonal pattern of (left panels) daily riparian evapotranspiration rates simulated for different climate change scenarios and (right panels) difference in the simulated values of daily riparian evapotranspiration between the reference period (1981–2000) and future climate scenarios (2081–2100). All the climate change scenarios were based on the 0.5 percentile of the Representative Concentration Pathway (RCP) projections provided by IPCC (2013) for the period 2081–2100 (Table 2): (a,b) RCP 2.5 (the most moderate scenario), (c,d) RCP 4.5, (e,f) RCP 6.0, and (g,h) RCP 8.5 (the most extreme scenario). Black lines are mean values and grey shadows indicate the maximum–minimum range of values simulated for the 20-years period. The red line in the left panels is the mean daily values of riparian ET for the reference period. The horizontal line in the right panel is shown as a reference.



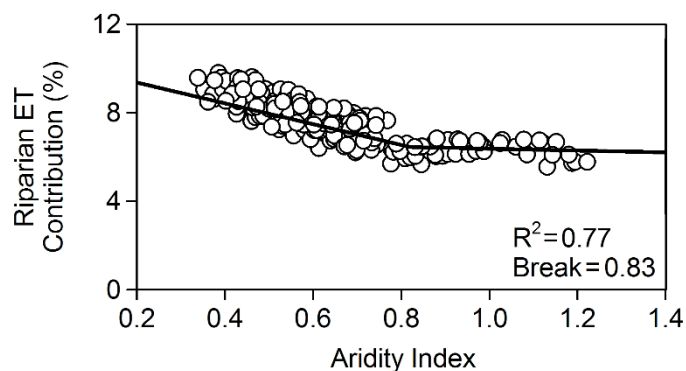


**Figure 6** Relationship between the relative contribution of riparian evapotranspiration (ET) to annual catchment water depletions and the aridity index for all the projections simulated with PERSiST as well as for the reference period. Total water output fluxes from the catchment (water depletions) are the sum of stream flow, upland ET, and riparian ET. The aridity index is the ratio between annual precipitation and potential evapotranspiration (P/PET). The goodness of fit of the two segment linear model and the break point are also shown.

635

640